

Measurement of the half-life of ^{163}Ho

P. A. Baisden, D. H. Sisson, S. Niemeier, and B. Hudson
Lawrence Livermore National Laboratory, Livermore, California 94550

C. L. Bennett and R. A. Naumann
Department of Physics, Princeton University, Princeton, New Jersey 08540
(Received 15 February 1983)

In a continuing effort to explore electron-capture decay properties of ^{163}Ho as a means of measuring the mass of the neutrino, we measured a half-life of 4570 ± 50 yr (95% confidence level) for ^{163}Ho using isotope-dilution mass spectrometry. From this value of the half-life we infer an electron-capture Q value of approximately 2.65 keV using known atomic physics factors and an estimate of the nuclear matrix element based on the systematics of electron-capture ft values of other Ho isotopes.

RADIOACTIVITY ^{163}Ho , electron capture decay, measured $T_{1/2}$, deduced Q
value.

Recently Lubimov *et al.* reported evidence for a nonzero neutrino rest mass.¹ They deduced a neutrino mass of $14 \leq m_\nu \leq 46$ eV (99% confidence level) from measurements of the high-energy portion of the β -decay spectrum of tritium substituted in a valine molecule. Because of the importance of this result, we began a reexamination of the electron-capture decay properties of ^{163}Ho specifically relevant to the measurement of the neutrino mass. This holmium isotope is especially interesting because the electron capture Q value ($Q_{\text{EC}} = 2.6 \pm 2.1$ keV), though quite uncertain, is unusually small.^{2,3} As a result, only EC from M (2.05 keV) or higher shells is energetically feasible. In an earlier paper,⁴ we reported the x-ray spectrum of ^{163}Ho following M capture. Because we observed $M1$ lines in our spectrum, we were able to set a lower limit on the Q value of 2.05 keV. Thus only $0.55^{+2.10}_{-0.55}$ keV of energy is available for the emerging neutrino. We report here our measurement of the half-life of ^{163}Ho and describe its relevance to neutrino mass experiments.

The ^{163}Ho used for the half-life measurements was prepared by neutron activation of an enriched ^{162}Er target by the reaction $^{162}\text{Er}(n,\gamma)^{163}\text{Er} \xrightarrow{\text{EC}} ^{163}\text{Ho}$ at the high-flux-beam reactor (HFBR) at Brookhaven National Laboratory. After irradiation, the erbium target was dissolved and Ho was chemically separated using high-pressure ion-exchange chromatography with α -hydroxyisobutyric acid as the eluant. Two such separations were required to reduce the erbium content in the holmium fraction to an acceptable level (< 1 ng). The elution peak of the holmium fraction was identified by counting $^{166}\text{Ho}^m$, which was probably produced by the (n,γ) reaction on traces of natural ^{165}Ho in the erbium target material.

The rate of ingrowth of stable ^{163}Dy from ^{163}Ho was measured by isotope-dilution mass spectrometry. Since the ^{163}Ho half-life appeared uncertain by orders of magnitude, we began by obtaining a rough, but much better, half-life estimate in order to determine the optimal amount of Dy tracer to add to the ^{163}Ho solution. In this preliminary work we determined the half-life to be roughly 6000 yr. Next, to avoid uncertainties associated with the chemical yield of dysprosium in the separation procedure, a known amount of an enriched ^{164}Dy spike solu-

tion was added to the parent ^{163}Ho fraction. Aliquots of the parent solution were withdrawn periodically, the dysprosium chemically isolated, and its isotopic composition measured by mass spectrometry. From the change in the $^{163}\text{Dy}/^{164}\text{Dy}$ ratio as a function of time, we determined the rate of ingrowth of daughter ^{163}Dy , from which the half-life of ^{163}Ho is calculated.

Solutions of natural Dy, natural Ho (monoisotopic ^{165}Ho), and isotopically enriched ^{164}Dy ($^{163}\text{Dy}/^{164}\text{Dy} = 0.01066$) were prepared by weight from high purity oxides. To reduce effects of nonstoichiometry and sorbed gases, all oxides were fired at 1100°C in air until a constant weight was achieved. The ^{164}Dy spike solution was calibrated against the natural Dy solution. The ^{163}Ho content of our parent fraction (0.735 ± 0.005 mg) was determined by two independent isotope dilution measurements using the natural Ho solution.

Four aliquots (each about 10% of the solution) were drawn from the parent fraction at times ranging from 15 to 132 d. For these intervals, we expected an ingrowth of radiogenic ^{163}Dy of between 3 and 9 ng/aliquot. The aliquots were separated into Ho and Dy fractions using chromatographic ion exchange. The holmium elution peak was identified as before from the presence of $^{166}\text{Ho}^m$. Since the dysprosium fraction did not contain a radioactive tracer, its peak position was determined by comparing the holmium peak position with a column-calibration run using the radioactive tracers $^{166}\text{Ho}^m$ and ^{159}Dy . On the basis of the calibration run, and by isotope dilution measurements of the actual samples, we determined that the amount of holmium remaining in the dysprosium fraction after one column separation was about one part in 20000 of the original holmium loaded on the column. Consequently, after one column separation, the amounts of ^{163}Ho and ^{163}Dy in the dysprosium fraction were roughly equal.

The dysprosium fraction from the first column was split into two aliquots. To one aliquot was added a small amount of isotope separated $^{166}\text{Ho}^m$. This sample was then separated by ion exchange to yield a second set of holmium and dysprosium fractions. All four fractions for each aliquot were further processed to remove the α -hydroxyisobutyrate, by lowering the pH to 2.0 and adsorb-

ing the holmium or dysprosium on a small cation column. After passing several milliliters of water through the column, the rare-earth ions were stripped from the resin using 6M HCl.

The entire chemical procedure was repeated several times in the absence of an actual sample, in order to determine the contribution of rare-earth ions from our ion-exchange resin and reagents. Analyses of these blank runs indicated that such contributions were about 200 pg or less.

After evaporating the dysprosium fractions to dryness, they were dissolved in a small volume of 6M HCl and loaded on V-shaped tantalum filaments. The samples were again evaporated to dryness and briefly oxidized by bringing the filament to a barely visible red glow. The samples were analyzed at Lawrence Livermore National Laboratory (LLNL) on MS-XL, a thermal ionization mass spectrometer with tandem 60° magnetic sectors of 34 cm radius and an electron multiplier operated in a pulse-counting mode for ion detection. Double filaments were used with the rhenium ionizing filament operated at about 2000 °C.

Considering the small samples involved (< 10 ng), non-trivial blank contributions to the signal were observed at the masses of interest (primarily 163, 164, and 165) arising from natural holmium, dysprosium, and neodymium (observed as NdO⁺). In addition, small traces of the enriched ¹⁵⁸Dy target material used to produce the ¹⁵⁹Dy tracer were observed in the last three aliquots. However, by acquiring data from masses 159 to 166, the contribution from each component could be uniquely and accurately determined. Decomposition of the data, as discussed below, was accomplished using a published NdO composition⁵ and our measured compositions for natural dysprosium and the ¹⁵⁹Dy tracer.

First, NdO is subtracted using the 160-161-162 systematics. The data can be resolved into their three constituents (NdO, natural dysprosium, and ¹⁵⁹Dy tracer) using standard techniques of partitioning three components of known composition by means of two particular observed isotopic ratios. All computations recognize that the uncertainties propagated in these calculations are frequently partially correlated; otherwise, the errors would be significantly and erroneously inflated. The algorithms and computer programs are described by Hudson.⁶

Next, the ¹⁶³Ho contribution is subtracted assuming that all of the 165 signal was due to holmium. The potential interferences from NdF and SmO were absent, as verified by periodic scanning of the 165–170 mass region. Because our samples contained less than 5 ng of ¹⁶³Ho, the

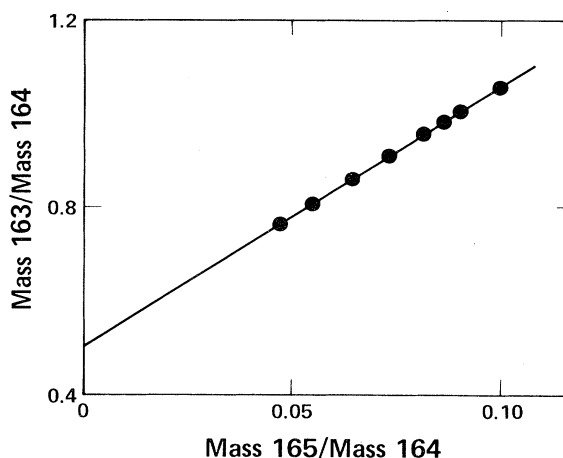


FIG. 1. Observed signals at masses 163–165 plotted as (163/164) vs (165/164) for data collected at different times during the mass spectrometric analysis of a dysprosium sample obtained after only one column separation. The uncertainty in the value of the intercept, which reflects the uncertainty in the ¹⁶³Ho correction, is approximately 0.1%.

¹⁶⁵Ho/¹⁶³Ho ratio of 0.1304 in the parent sample was significantly altered by variable ¹⁶⁵Ho-blank contributions. Nevertheless, this ratio can be determined for each particular aliquot since the relative signals from dysprosium and holmium varied with time during the data acquisition (dysprosium comes off the filament first). In Fig. 1, the 163/164 ratio is plotted against the 165/164 ratio (after subtracting NdO contributions) for the data collected at different times during the mass spectrometric analysis of a dysprosium sample obtained after only one column separation. This sample represents a worst-case situation with respect to holmium contamination in the dysprosium fraction. In this graph, data points generated by variations in the relative signals from two components will lie on the line segment connecting their compositions. Thus the linear correlation seen in Fig. 1 is interpreted as a binary mixture of holmium and dysprosium. Since holmium does not contribute to the 164 signal, the slope of the correlation line corresponds to the ¹⁶³Ho/¹⁶⁵Ho ratio. To enhance the accuracy of the ¹⁶³Ho subtraction, we increased the ¹⁶⁵Ho/¹⁶³Ho ratio in most of the samples to approximately unity by adding ¹⁶⁵Ho.

Following the ¹⁶³Ho subtraction, natural dysprosium and ¹⁵⁹Dy tracer contributions to the 163 and 164 signals are subtracted using the known compositions and the earlier decomposition. At this point the 164 signal is attri-

TABLE I. Decomposition results (%). A blank entry indicates that no contribution from a given component is possible at that mass number.

Component	Aliquot 1		Aliquot 2		Aliquot 3		Aliquot 4	
	163	164	163	164	163	164	163	164
NdO		2		2		0.3		3.3
Ho	43		5		8		27	
^{nat} Dy	4	4	6	6	5	4	4	4.6
¹⁵⁹ Dy tracer	0	0	29	3	4	0.4	1	0.1
¹⁶⁴ Dy spike	1	94	1	89	1	95.3	1	92
¹⁶³ Dy*	52		59		82		67	

butable entirely to the $^{164}\text{Dy}_{\text{spike}}$, and the 163 signal is predominantly radiogenic $^{163}\text{Dy}^*$ plus a small contribution from the $^{164}\text{Dy}_{\text{spike}}$. After correcting the 163 signal for the spike component, we obtained the desired ratio of $^{163}\text{Dy}^*/^{164}\text{Dy}_{\text{spike}}$.

The relative contribution of each component is shown in Table I for the four aliquots used in the determination of the half-life. The four aliquots not shown were disregarded due to much poorer quality data. The average contribution to the 164 signals are fairly similar for all aliquots, with the $^{164}\text{Dy}_{\text{spike}}$ accounting for $\geq 90\%$ of the signal. For the 163 signals, however, the interfering components range from 18% to 48% of the total signal, and the relative contributions also show a much greater variation. The Ho contributions in aliquots 2 and 3 are substantially smaller because two column separations were performed for these aliquots, whereas aliquots 1 and 4 had only one separation. The contribution from the ^{159}Dy tracer is by far the greatest in aliquot 2, which was separated just after the column calibration. The subsequent decreases in the tracer levels were due to a cleanup effort which included replacement of much of the column apparatus. Natural Dy contributions are fairly constant and are consistent with our procedural blank levels.

During the course of an analysis, the isotopic composition of an element will vary slightly due to mass fractionation. Although these effects were not explicitly taken into account in the above decomposition, we can estimate the significance of these effects from observed mass fractionations in elementally clean samples. Analyses of the Dy standard and Ho parent solution indicate that the total width of the isotope ratio distribution generated by mass fractionation is typically $\sim 0.3\%$ for both Dy and Ho. The uncertainties introduced by these fractionations for

the NdO and various Dy components are actually smaller than this total range, since for all samples we maintained approximately the same beam intensity as a function of time during the analysis. But this is not true for the Ho correction since the 163/165 ratio is deduced from the slope of a line as shown in Fig. 1. Thus, the Ho correction to the 163 signal may be overestimated by as much as 0.6%.

With respect to the half-life of ^{163}Ho , the ingrowth of $^{163}\text{Dy}^*$ is a linear function of time over the duration of our experiment. The measured $^{163}\text{Dy}^*/^{164}\text{Dy}_{\text{spike}}$ ratios are plotted as a function of time in Fig. 2. On the lower portion of the figure, the errors are within the size of each point; the upper portion shows the percent deviation from the least squares line. The statistical uncertainty for each point is considerably smaller than the indicated errors, since the assigned errors reflect our estimate of both the uncertainties introduced by mass-fractionation effects during an analysis and the systematic errors in the subtraction of the interfering components. In the figure, $t=0$ corresponds to the time of separation of dysprosium from the entire holmium fraction.

Assuming that all the Dy was removed from the holmium fraction at $t=0$, the data points should lie on a straight line passing through the origin. A least squares line fit to the four measured data points gives a slope of $1.286 \pm 0.040 \text{ yr}^{-1}$ and an intercept of 0.0068 ± 0.00176 (all errors are 95% confidence limits). The least-squares fit takes into account errors on both coordinates and allows for correlations between the two errors.⁷ Since the intercept is indistinguishable from zero, we have constrained the least squares line to pass through the origin. With this constraint we obtain a slope of $1.300 \pm 0.006 \text{ yr}^{-1}$. The degree to which the points fit the line in Fig. 2 suggests that the uncertainties assigned in the decomposition procedure are approximately correct. The possibility of a significant systematic error, which nonetheless preserves a good fit, seems unlikely in view of the substantially different corrections among the four aliquots. The Fig. 2 graph does not take into account the possible systematic effect of Ho mass fractionation, but if the Ho correction were adjusted by 0.6%, the goodness of fit would be improved and the slope would be lowered by only 0.2%.

The slope corresponds to the rate of change of $^{163}\text{Dy}^*$ relative to the $^{164}\text{Dy}_{\text{spike}}$ as a function of time. Combining this with the ratio of ^{163}Ho to $^{164}\text{Dy}_{\text{spike}}$ in the parent fraction gives the half-life

$$t_{1/2} = \frac{\ln 2}{\text{slope}} \times \frac{^{163}\text{Ho}}{^{164}\text{Dy}_{\text{spike}}}$$

For a slope of 1.300 yr^{-1} , $t_{1/2} = 4570 \pm 50 \text{ yr}$, where the uncertainty is dominated by the uncertainty in the ^{163}Ho to $^{164}\text{Dy}_{\text{spike}}$ ratio. Our results are slightly outside the limits of the recently reported half-life estimate of $7000 \pm 2000 \text{ yr}$ of Andersen *et al.*,⁸ but this difference is easily understood in view of the fact that their half-life was deduced from a difficult measurement of the partial half-life for M capture and theoretical ratios for $M/N/O$ capture. Our measurement, on the other hand, constitutes a direct determination of the half-life.

Given the total ^{163}Ho half-life, the EC Q value can be calculated from the following relation⁹:

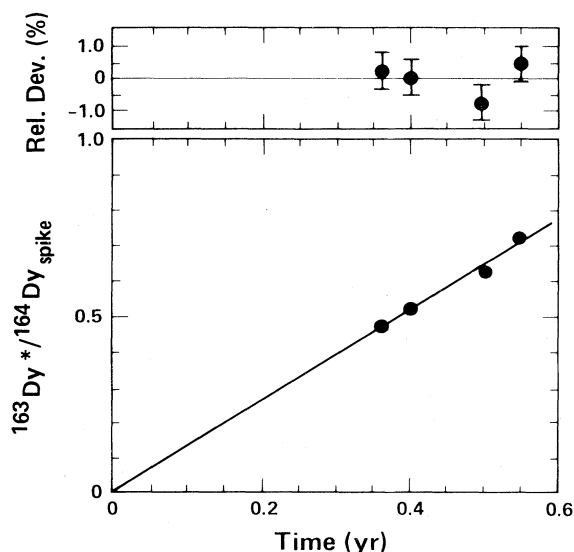


FIG. 2. Time evolution of radiogenic $^{163}\text{Dy}^*$ to $^{164}\text{Dy}_{\text{spike}}$. In the upper portion of the figure, relative deviations from the regression line are shown; errors are 2σ . The slope of the line (constrained to pass through the origin) is $1.300 \pm 0.006 \text{ yr}^{-1}$. This value combined with the ratio of ^{163}Ho to $^{164}\text{Dy}_{\text{spike}}$ in the parent sample ($= 8.574 \times 10^3$, atomic) gives a half-life of $4570 \pm 50 \text{ yr}$.

$$\lambda_{\text{total}} = \sum_i \lambda_i = \frac{g^2}{4\pi^2} |M|^2 \sum_i n_i B_i \beta_i^2 q_i w_i,$$

where g is the weak interaction coupling constant and $|M|$ is the nuclear matrix element. For electron state i , n_i is the occupation probability, B_i is the overlap and exchange correction, β_i is approximately the electron wave function amplitude over the nuclear volume, and q_i and w_i are the momentum and total energy, respectively, of the neutrino. For $m_\nu = 0$, $q_i = w_i = (Q_{\text{EC}} - E_i)$, where E_i is the binding energy of the i electron in the daughter atom.

In order to compute Q_{EC} , we need to know $|M|^2$, n_i , β_i , and B_i . In general, the quantities n_i , β_i , and B_i depend on the properties of bound atomic states, common to all isotopes of the same element, and as such are known with a fair degree of confidence.^{9,10} Consequently, the reliability with which we can determine Q_{EC} rests primarily on our estimate of $|M|^2$.

We can obtain values of $|M|^2$ for ¹⁵⁷Ho, ¹⁵⁹Ho, and ¹⁶¹Ho using measured values of Q_{EC} , $t_{1/2}$, and a branching ratio for the $\frac{7}{2}[523]$ to $\frac{5}{2}[523]$ electron capture transition for each isotope.³ Figure 3 shows a graph of $|M|^2$ (normalized to $|M|^2 = 1$ for ¹⁶¹Ho) as a function of mass number. The uncertainties indicated for $|M|^2$ are based on the uncertainties in Q_{EC} and $t_{1/2}$ only. The constancy of the electron capture rates, as reflected by the similar values of $|M|^2$ calculated for ¹⁵⁷,¹⁵⁹,¹⁶¹Ho, suggests that $|M|^2(^{163}\text{Ho}) \approx |M|^2(^{161}\text{Ho})$.

If, instead, we use the single particle Nilsson model with pairing correlation¹¹ to extrapolate $|M|^2$ from the lighter

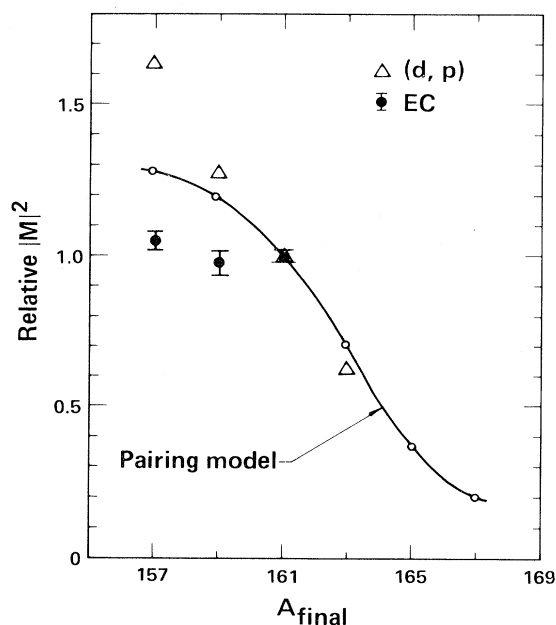


FIG. 3. Relative values of $|M|^2$ as a function of mass number obtained from the electron capture decay of ¹⁵⁷Ho, ¹⁵⁹Ho, and ¹⁶¹Ho involving the $\frac{7}{2}[523]$ to $\frac{5}{2}[523]$ transition are shown as (●). Also included are the relative $|M|^2$ derived from a (d,p) reaction on even mass Dy isotopes populating the $\frac{5}{2}[523]$ neutron state (△). The variation of $|M|^2$ with mass as predicted by the pairing model is shown as the solid curve. All values of $|M|^2$ have been normalized to $|M|^2 = 1$ for ¹⁶¹Ho.

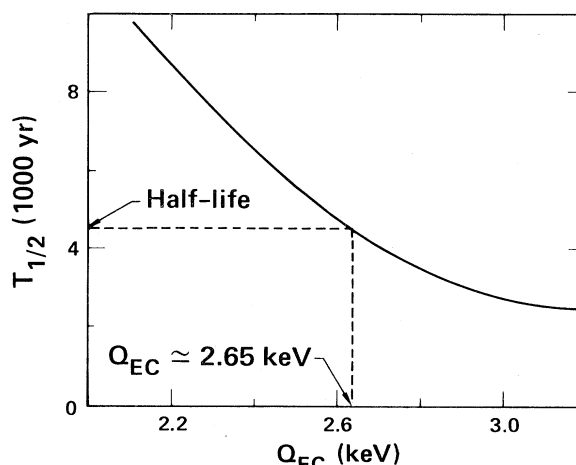


FIG. 4. The expected variation of half-life ($T_{1/2}$) with the electron capture Q value assuming $|M|^2(^{161}\text{Ho}) = |M|^2(^{163}\text{Ho})$ is shown as the solid curve. The measured $T_{1/2}$ of 4570 yr implies a Q_{EC} of approximately 2.65 keV.

isotopes (as done by Andersen *et al.*⁸), we obtain the solid curve shown in Fig. 3 which gives $|M|^2(^{163}\text{Ho}) \approx 0.7 |M|^2(^{161}\text{Ho})$. We point out that the application of the pairing model is questionable in this case since it presumes that the proton and neutron orbits have only a weak interaction compared to the pairing energy. In the case of an allowed unhindered transition like ¹⁶³Ho \rightarrow ¹⁶³Dy, the proton and neutron states have very similar spatial wave functions differing primarily by the coupling of the nuclear spin to the orbital angular momentum. Thus the possibility for significant proton-neutron interaction exists, contrary to the premise of the pairing model.

We can also examine (d,p) direct transfer reactions for the even A Dy isotopes where a Nilsson $\frac{5}{2}[523]$ neutron is created. In terms of the pairing model, $|M|^2$ for the $\frac{7}{2}[523]$ proton orbit to the $\frac{5}{2}[523]$ neutron orbit is proportional to the vacancy factor u^2 for the $\frac{5}{2}[523]$ neutron state. Likewise, the (d,p) cross sections, when adjusted for Q -value differences, are also proportional to u^2 . However, the relative (d,p) cross sections shown in Fig. 3 show a much steeper, more linear decrease with increasing A than predicted by the pairing model.¹²

The relation between the (d,p) cross sections and $|M|^2$ is more general than the pairing model provided that the (d,p) reaction really is a direct single nucleon transfer. However, experimentally it is found that the (d,p) reaction on the Dy isotopes to the state of interest, $\frac{5}{2}[523]$, has a very small cross section and may not be excited by a direct reaction mechanism.¹³ Thus neither the pairing model nor (d,p) cross sections provide a suitable estimate for $|M|^2$ and we have adopted $|M|^2(^{163}\text{Ho}) = |M|^2(^{161}\text{Ho})$ based on the lack of variation of $|M|^2$ derived from EC ft values in other Ho isotopes. The absolute value of the nuclear matrix element is then calculated from published values for $t_{1/2}$, Q_{EC} , and the atomic physics factors for ¹⁶¹Ho.

Using this value of the matrix element, the relation between $t_{1/2}$ and Q_{EC} for ¹⁶³Ho is shown in Fig. 4. The measured half-life of 4570 yr implies a Q_{EC} of approxi-

mately 2.65 keV. We emphasize that the value of the nuclear matrix element enters critically in the determination of Q_{EC} , as an uncertainty of $\pm 30\%$ on the matrix element corresponds to a Q_{EC} range of 2.45–2.90 keV. This determination is in good agreement with the value of 2.58 keV estimated by Andersen *et al.*⁸ from measurements of the partial half-life for capture of M electrons.

In our previous paper⁴ we pointed out that a Q_{EC} value of 2.6 keV would require a precision of 0.04% for measurements of relative capture rates from different electron orbits in order to establish a neutrino mass of 35 eV at the 1σ confidence level. Thus the Q_{EC} value reported here makes this approach impractical. However, we believe the resonant enhancement of the inner bremsstrahlung spec-

trum¹⁴ can be exploited to detect an electron-neutrino mass as low as 35 eV.

The authors gratefully acknowledge the valuable assistance of R. Chrien and the staff of the HFBR at the Brookhaven National Laboratory for the neutron irradiation. In addition, we note our appreciation for the contributions of J. Meadows, G. P. Russ, D. A. Leich (Lawrence Livermore National Laboratory), and P. Springer (Princeton University) in the early stages of this work. This work was performed under the auspices of the U.S. Department of Energy by the Lawrence Livermore National Laboratory under contract number W-7405-ENG-48.

¹V. A. Lubimov, E. G. Novikov, V. Z. Nozik, E. F. Tretyakov, and V. S. Kosik, *Phys. Lett.* **94B**, 266 (1980).

²P. K. Hopke, J. S. Evans, and R. A. Naumann, *Phys. Rev.* **171**, 1290 (1968).

³*Tables of Isotopes*, 7th ed., edited by C. M. Lederer and V. S. Shirley (Wiley, New York, 1978).

⁴C. L. Bennett, A. L. Hallin, R. A. Naumann, P. T. Springer, M. S. Witherell, R. E. Chrien, P. A. Baisden, and D. H. Sisson, *Phys. Lett.* **107B**, 19 (1981).

⁵G. J. Wasserburg, S. B. Jacobsen, D. J. DePaulo, M. T. McCullough, and T. Wen, *Geochim. Cosmochim. Acta* **45**, 2311 (1981).

⁶B. Hudson, Ph.D. thesis, Washington University, St. Louis, Missouri, 1981.

⁷D. York, *Earth Planet. Sci. Lett.* **47**, 211 (1969).

⁸J. U. Andersen, G. J. Beyer, G. Charpak, A. De Rujula, B. El-

bek, H. A. Gustafsson, P. G. Hansen, B. Jonson, P. Knudsen, E. Laegsgaard, J. Petersen, and H. L. Ravin, *Phys. Lett.* **113B**, 72 (1982).

⁹W. Bambynek, H. Behrens, M. H. Chen, B. Crasemann, M. L. Fitzpatrick, K. W. D. Ledingham, H. Genz, M. Mutterer, and R. L. Intemann, *Rev. Mod. Phys.* **49**, 77 (1977).

¹⁰I. M. Band and Vi. I. Fomichev, *At. Data Nucl. Data Tables* **23**, 296 (1979).

¹¹A. Bohr and B. R. Mottelson, *Nuclear Structure* (Benjamin, Reading, Mass., 1975), Vol. II, p. 263ff.

¹²T. Grotdal, K. Nybo, and B. Elbek, *K. Dan. Vidensk. Selsk. Mat.-Fys. Medd.* **37**, 1 (1970).

¹³P. Holan, M. Rozkos, F. Sterba, and J. Cejpek, *Czech. J. Phys.* **D24**, 395 (1974).

¹⁴A. De Rujula, *Nucl. Phys.* **B188**, 414 (1981).